Article:
Waters, I, Jones, D orcid.org/0000-0002-2961-8483, Alazmani, A orcid.org/0000-0001-8983-173X et al. (1 more author) (2022) Utilising Incipient Slip for Grasping Automation in Robot Assisted Surgery. IEEE Robotics and Automation Letters, 7 (2). pp. 1071-1078. ISSN 2377-3766

https://doi.org/10.1109/lra.2021.3137554

Utilising Incipient Slip for Grasping Automation in Robot Assisted Surgery

Ian Waters[1], Dominic Jones[2], Ali Alazmani[1] and Peter Culmer[1]

***Abstract*—Despite recent advances in modern surgical robotic systems, an ongoing challenge remains their limited ability to control grasp force. This can impair surgical performance as a result of either tissue slippage or trauma from excessive grasp force. In this work we investigate a force control strategy to address this challenge based on the detection of incipient slip. Our approach employs a grasper face whose shape is engineered to encourage preferential localised slips that can be sensed using embedded displacement sensors prior to gross slip occurring. This novel approach enables closed loop control of the grasping force to prevent gross slip whilst applying minimal force. In this paper we first demonstrate the efficacy of sensing incipient slip and then demonstrate how this can form a robust closed loop grasping system to maintain stable control of tissue. Results demonstrate that this approach can achieve equivalent grasping performance to a scheme employing a fixed maximal grasping force while reducing tissue loading, and thus risk of trauma. This provides the foundation for the development of automated surgical robots with adaptive grasp force control.**

***Index Terms*—Surgical Robotics: Laparoscopy, Grasping, Force Control**

I. Introduction

THE introduction of robotic surgical devices has helped advance Minimally Invasive Surgery (MIS) and has lead to improved surgical outcomes [1]. However their limited grasping force control while handling soft tissue remains an issue and is the cause of a significant number of surgical errors [2], [3]. This can be due to either the over application of force, leading to tissue trauma [2], or a lack of clamping load resulting in adverse slip events during surgical procedures [3].

Haptic feedback of grasping forces has been demonstrated as a viable technique to minimise the occurrence of tissue trauma due to excessive clamping loads [4], [5], [6]. However this requires the surgeon to continually monitor and maintain an appropriate applied grasping load (neither too high or too low), a task which is both challenging and can incur an increased cognitive load [7]. An alternative strategy can be formed through inspection of tissue movement at the grasper face, rather than the applied load. Specifically, through detection and monitoring of tissue slip, the clamping force can be adjusted to use the minimum force required to prevent slip events from occurring, whilst minimising the occurrence of tissue trauma. This control method also provides the opportunity for a grasping automation method which is independent of tissue properties, helping to reduce surgeon fatigue and allowing a focus on more critical higher-level tasks [8].

A range of approaches have been proposed for using slip as the basis for automated surgical grasping. Using a predefined *'safe grasping zone'* allows regulation of grasping force as a function of detected shear, aiming to use the minimum force required to prevent slip [9]. However this requires tissue-specific safe zones to be prescribed, limiting clinical utility. More adaptive approaches have utilised sensors embedded within the grasper face to monitor tissue shear against it. Jones *et al.* [10] used a two-axis soft inductive tactile sensor to monitor normal and shear forces at the grasper face, determining slip as the point when the coefficient of friction first peaks. Burkhard *et al.* [11] developed a novel slip sensing method using hot wire anemometer techniques to monitor changes in heat flux through the tissue. The system was able to effectively detect slip during small movements in tests on porcine tissue.

Slip events during grasping can be broken down into two stages; first *incipient slip* followed by *macro slip* [12]. During incipient slip the total shear force across the contact is less than the total friction force, thus overall the contact is held securely [12]. However the friction force may vary in localised areas across the contact surface and where this is exceeded by the shear friction then localised movement will occur, these are termed 'incipient slips' [12]. As the total shear force increases these incipient slip events will increasingly occur. When the total shear force exceeds the total friction the contact will enter a macro slip regime and grip stability is lost [12].

The slip sensing approaches described above detect the occurrence of macro slip, and so require a loss of grip control to occur before mitigating actions can be taken. An alternative approach is to focus on the detection of incipient slip, allowing slip events to be identified early and grip control to be maintained throughout the retraction process. Detection of incipient slip has been utilised by the wider robotics community for grasping control, but has seen limited application in the field of surgical robotics or in the grasping of deformable materials. The only example is reported by Stoll *et al.* [13] who developed a system based on monitoring the global shear force to determine material stiffness, and thus the early onset of macro slip. The technique was found to be effective but only provides a limited time window in which to

This work was supported by the Engineering and Physical Sciences Research Council (EPSRC) under grant EP/R513258/1 and supported by the National Institute for Health Research (NIHR)

[1]I.Waters, A.Alazmani and P.Culmer are with the School of Mechanical Engineering, University of Leeds, United Kingdom. (mn10iw@leeds.ac.uk, A.Alazmani@leeds.ac.uk, P.R.Culmer@leeds.ac.uk)

[2]D.Jones is with the School of Electronic and Electrical Engineering, University of Leeds, United Kingdom

prevent macro slip.

In developing a sensor to detect incipient slip a key aspect is to encourage these local slip events to occur in a consistent and repeatable manner [14]. Biomimicry of the human finger has been used by many as inspiration; typically employing a curved finger-like surface to create a normal force distribution, and thus corresponding variation of frictional force, across the contact surface [14], [15], [16]. This approach has been demonstrated as a viable method for encouraging the incipient slip of lubricated and deformable materials similar to soft biological tissues [17]. Khamis *et al.* [18] investigated an alternative to using a continuous curved surface to control friction forces, instead using an array of stepped pillars to create discrete variations in height and thus normal force. Overall, incipient slip sensors typically use similar methods for varying frictional forces across the contact surface to encourage incipient slip, but they employ a range of sensing modalities to detect the occurrence of these slips, including measurement of vibration, normal force distribution, shear force magnitude, contact area or optical imaging, a detailed evaluation of these is provided in a recent review by Chen *et al.* [14].

Our research aim is to build on the incipient slip sensing methods developed across the wider robotics community for use within a surgical robotic system. This paper reports the design of an incipient slip sensor system that employs a curved grasper profile to encourage and detect the occurrence of incipient slip in deformable and lubricated tissue-like materials. We then propose a method for the automated detection of incipient slip events using this sensor and evaluate its ability to prevent the occurrence of gross slip events under representative surgical conditions. The novelty of this work is the use of incipient slip mechanics, in a physical sensing system, for early prediction (and thus avoidance) of gross slip during the grasping and manipulation of soft-tissue like materials. This has particular relevance in the automation of surgical grasping.

II. System Development

A. Concept and Requirements

The core requirement of this sensing system was to induce measurable levels of incipient slip in tissue during surgical grasping conditions. We approached this using a concept which employs a curved grasping surface that is segmented into independently mobile sections. The curved surface causes higher frictional forces to occur in the middle of the grasper in comparison to the edges, thus encouraging slip to occur in the outer sections of the grasper prior to the middle [17] as illustrated in (Fig. 1). Using this approach, it is possible to detect incipient slip by measuring the relative displacement of the independent 'island' sections. Consider a typical retraction movement; during the initial stages the shear force is low and friction forces dominate, such that the outer and middle islands will move together with the tissue. As retraction continues, shear forces will increase (e.g. by pulling tissue), beginning to exceed frictional forces at the outer edges, thus tissue slip will occur and the outermost islands will move less than the middle island. Consequently, monitoring the differential relationship between outer and middle island's movement provides the means to detect incipient slip.

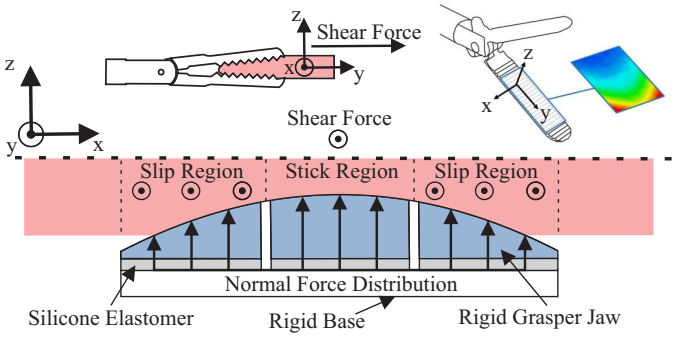

Fig. 1: Diagram demonstrating the concept of encouraging incipient slip across independently moveable section of the grasper face through the variation of normal force using a curved surface.

B. System Design and Fabrication

To evaluate this sensor concept, a scaled prototype was developed and realised. Based on preliminary work [17], a curved grasper face with a radius of 100.25 mm was separated into a 5×3 grid of islands as shown in Figure 2, providing islands spanning the width and length of the grasper face. Islands were separated along the length of the grasper to isolate them from the effect of slip propagation between the front and back of the grasper caused by the elastic properties of the tissue [17].

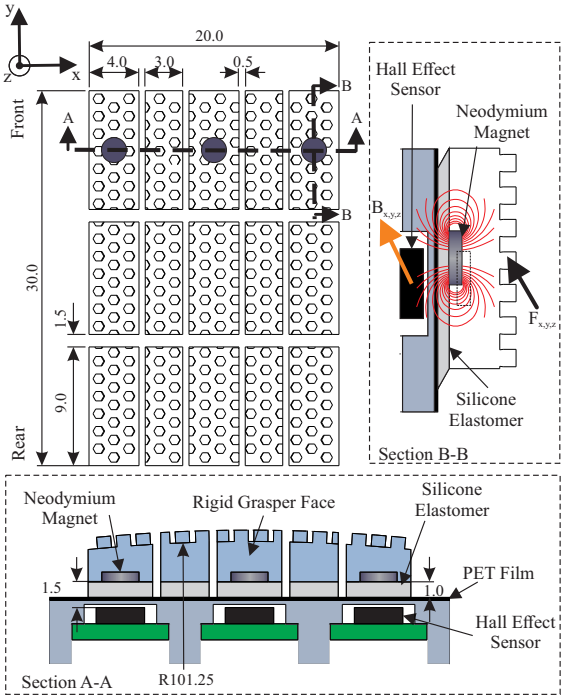

Fig. 2: Dimensioned drawing of the grasper separated into 5×3 grid of independently moveable islands, the gray circles indicate the positions of the sensing nodes (All dimensions in mm). Section A-A: cross section across the width displaying the design of the sensored and passive islands. Section B-B: Principle of operation of the sensing system, displaying how the magnetic field moves through the Hall effect sensor as force is applied to the island.

Each island comprises a 3D printed upper rigid face (Rigid 4000 Resin, Formlabs) to provide the gripping surface, and a 1 mm thick silicone elastomer base (Ecoflex 00-30, Smooth-on) to allow independent movement of the rigid face. The islands were then attached to a PET film on a rigid base. The grasper faces featured a regular hexagonal pattern (0.75 mm width, height and separation) to provide an isometric gripping surface suited to soft deformable materials [17], [19].

Prior work characterised the mechanical behaviour of the system under representative loading conditions and thus define the underlying sensor requirements [17]. The relative difference in tissue displacement at the point of incipient slip between the outer and middle of the curved grasper was found to lie within a range of 0.1-0.2 mm [17]. The sensing elements also need to be sufficiently compact to fit across the width of the grasper. To meet these requirements, a Hall effect based tactile sensing method was used. Each element consists of a three-axis Hall effect sensor chip (MLX90393, Melexis) coupled with a neodymium disc magnet (2 mm diameter $\times$ 0.5 mm thick) embedded in the base of the grasper islands (see Fig. 2). When a force ($F_{x,y,z}$) is applied to the grasper face the elastomer layer deforms such that the island's gripping surface and magnet change position relative to the Hall effect sensor. The magnetic field at the sensor ($B_{x,y,z}$) can then be calibrated and converted into a corresponding displacement. For more details on the development of these tactile sensing elements see [20]. The array of sensing elements in the grasper was interfaced to a microcontroller (Teensy 3.6, PJRC) using the I^2C protocol and recorded at a sample rate of 100 Hz.

C. Signal processing

The sensors were calibrated using a custom three-axis sensor calibration system (detailed in [20]), to conduct a volumetric positioning sweep, moving in the x-y plane (-2 to 2 mm at 0.2 mm/s) for each z axis step (-0.65:1.25 mm in 0.1 mm increments) where {0,0,0} represents the island in an unloaded 'neutral' position. The measured magnetic field was calibrated to displacement using a neural network implemented using the Matlab neural net fitting toolbox (Matlab, Mathworks). A two-layer feed forward network configuration was selected as appropriate to represent the system based on prior work using a similar Hall effect sensor [20]. The overall network consisted of 40 neurons in the hidden layer and used a Bayesian regularization backpropagation algorithm as the training method to accommodate the non-linear relationship between magnetic field and displacement [20]. The trained neural network showed close correlation with validation data, with root mean squared errors of 0.029 mm, 0.025 mm and 0.018 mm, in x, y and z respectively. A third order Butterworth filter with a cut off frequency of 10 Hz was applied to the output of the neural network to attenuate high frequency noise in the displacement data.

D. Slip Detection & Mitigation

In the context of this work, incipient slip is defined as the event when one or more islands start to slip against the grasped tissue, whilst the majority maintain a stable grip. This manifests as a movement differential between these islands which can be detected by monitoring the displacement of the individual islands.

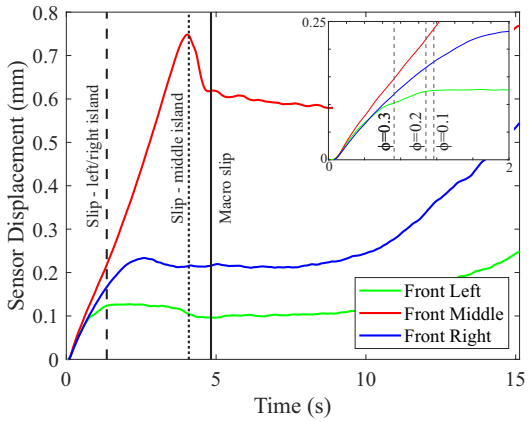

Fig. 3: Example of typical displacement characteristics for the front left, middle and right islands of the grasper under a 20N clamp load with a retraction speed of 2 mm/s (using Mat C). The inset shows how variation of the slip ratio changes when incipient slip of the edge islands is detected.

Applying these general criteria to the specific form of the instrumented grasper, detection of incipient slip relates to the outer (left and right) islands slipping relative to the central islands. This phenomenon is preferentially promoted through the curved design of the islands across the grasper face (see Fig. 1) such that tissue at the outside of the grasper has higher probability of slipping compared to central regions (due to differing normal loads) as increasing shear force is applied during retraction.

To automatically detect the presence of these incipient slips an algorithm was developed that is focused on the detection of slip during tissue retraction, when shear force is increasing, as this represents a 'worst-case' when slip is most likely to occur. Exploratory testing was conducted to investigate the parameter space and understand the sensor characteristics. Tests consisted of retracting a tissue simulant held by the sensor (with a configuration as shown in Fig. 6) up to the point of macro slip across a range of configurations consisting of: three clamp forces (10 N, 20 N, 30 N), three retraction speeds (1 mm/s, 2 mm/s, 5 mm/s), and three levels of tissue stiffness (Mat A - 241 kPa, Mat B - 320 kPa and Mat C - 610 kPa).

Figure 3 shows a typical example of the sensor response from these tests, revealing the differing displacement of the three instrumented islands over the course of a tissue retraction in which a simulant, Mat C, was grasped with a constant load of 20 N, and retracted at a constant speed of 2 mm/s. Across the parameter space, the sensor system showed this consistent general response: during the early stages of retraction (low shear loading), the middle and side islands move together with the same velocity. As retraction continues, the shear force increases and the left and right outer islands (where normal and thus frictional forces are lower) begin to slip against the tissue and their velocity decreases. This continues until movement of the outer islands stops, indicating complete slip against the tissue simulant in this region. Therefore, calculating the velocity (in the direction of shear) of the left (V_l) and right

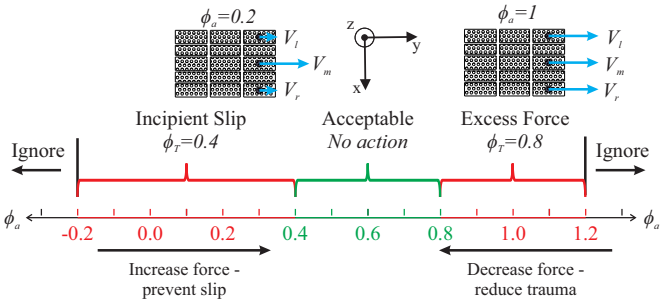

Fig. 4: A schematic showing the grasping and slip regimes defined by ϕ slip ratios and the associated response of the automated system. Uppermost, the diagrams show how the relative velocity of the islands, in the direction of retraction, differ in these regimes.

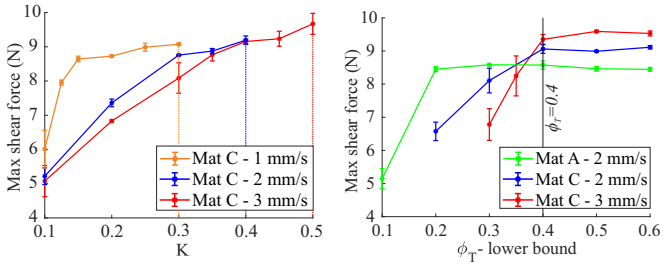

(a) (b)

Fig. 5: Graphs showing the effect on the shear force required to induce macro slip for the automated grasper during surgical retraction for: (a) Variation in gain. The dashed vertical lines indicate the gains identified for each retraction speed. (b) Variation of ϕ_T lower bound.

islands (V_r) as a ratio of the velocity of the middle island (V_m) defines their magnitude of slip with respect to the middle island. This ratio was thus termed the slip ratio (ϕ).

$$\phi = \mathbf{min}\left[\frac{V_l}{V_m}, \frac{V_r}{V_m}\right] \tag{1}$$

The physical embodiment of the slip ratio (ϕ) is presented in Figure 4. A slip ratio (ϕ) at or approaching 1 indicates the side and middle islands are moving together and there is no incipient slip. As ϕ decreases an increasing amount of relative slip is occurring between the tissue and the outer islands with respect to the middle. When ϕ reaches 0 there is no longer any motion of the outer island in the direction of shear, indicating that this region is slipping freely against the tissue as it is retracted. Informed by these preliminary investigations, $\phi < 0.2$ was identified as a reliable threshold to signify incipient slip of that island had occurred that was applicable across the full parameter space. This allows for robustness to noise (e.g. due to measurement or environmental factors), together with variability in the grasping conditions explored here.

A slip mitigation algorithm was developed based on the ϕ ratio, to adjust the grasping force as a function of the actual slip ratio, termed 'ϕ_a', and the retraction speed (a variable available in surgical robotic systems). The algorithm is based on maintaining ϕ_a within a desirable envelope in which the grip is 'stable'. The target slip ratio ϕ_T varies dependent on the current state of the system, as shown in Figure 4 and defined in Equation 2, where operating regions are defined around the incipient slip onset point of ϕ=0.2 with a safety factor of 2. Thus, for $\phi_a < 0.4$ the system should increase the grasping 'clamping' force to prevent slip occurring, but when $\phi_a > 0.8$ the system should reduce the grasp force to minimise tissue trauma as at this slip ratio there is only minimal relative slip occurring (no relative slip at $\phi_a = 1$). Between these two regimes ($0.4 \leq \phi_a \leq 0.8$) the grasp force should remain constant. Slip ratios which occur outside this range (e.g. due to low speeds as the island velocities approach zero) are considered anomalous and ignored.

$$\begin{aligned} \mathbf{If}\ \phi_a < 0.4\,,\ \phi_T = 0.4 \\ \mathbf{ElseIf}\ \phi_a > 0.8\,,\ \phi_T = 0.8 \end{aligned} \tag{2}$$

The grasping force to be applied $F_{c_{i+1}}$ during retraction is then determined using the equation:

$$F_{c_{i+1}} = F_{c_i} + K(\phi_T - \phi_a) \tag{3}$$

where the value of ϕ_T is determined based on the current value of ϕ_a as shown in Figure 4 and Equation 2, and the gain (K) varies as a linear function of the retraction speed of the linear stage(V_s).

$$K = 0.1V_s + 0.2 \tag{4}$$

Equation 4 was derived experimentally through inspection of the system response across three separate retraction speeds using Mat C (the stiffest material and thus most challenging case). A gain was identified for each retraction speed by progressively increasing K until it provided comparable grasping performance (i.e. the peak shear force occurring before macro slip) to a system operating at maximum clamp load, as shown in Fig. 5(a). These gains were then used to fit the linear function defined in Equation 4. The system operates at a sample frequency of 100 Hz.

N.B. This algorithm is only applied whilst $V_m > 0$ as this indicates firstly that there is tissue retraction occurring and secondly that the middle island is still securely gripping the tissue. If the middle island slips against the tissue ($V_m \leq 0$) the current algorithm is no longer applicable and so the grasp force remains constant.

Validation testing was conducted to ensure the slip onset threshold $\phi_T = 0.4$ was appropriate for a range of conditions. The automated grasping system described above was used at extremes of the parameter space (varying material and retraction speed) to find the resultant peak grasping load achieved. As shown in Fig. 5(b), increasing ϕ_T leads to initial increases in the peak shear force before the trend plateaus, a trend seen across the parameter space. From these data, using a fixed value of $\phi_T = 0.4$ for the slip threshold provides consistent performance across the parameter space which minimises dependence on material properties (information that is difficult to ascertain in advance).

III. System Evaluation

The system was tested to evaluate the efficacy of using an incipient slip sensor as the basis of an automated grasping control method. The performance of this system can be evaluated through its ability to prevent the occurrence of global

slip events whilst minimising the grasping force applied to the target specimen (to minimise trauma) under conditions representative of those used in surgical practice.

A. Experimental Set up and analysis

An experimental apparatus was configured to simulate the movements of surgical grasping and retraction, as shown in Figure 6. Tissue simulant samples were fixed to the endpoint of a linear load tester (Instron 5940, Instron) which was then used to control retraction movements. The grasping face with integrated sensing elements was mounted onto a pneumatic piston controlled via a pressure regulator (MGPM20TF-75Z, SMC, & ITV1030,SMC) to apply controlled grasp force. The grasp force was pre-calibrated using a reference load cell with the regulator. Shear force and retraction speed were measured by the linear load tester and recorded using a real-time embedded controller (MyRIO, National Instruments). This controller also interfaced with the grasping sensor through the microcontroller, and implemented the control algorithm to vary the clamp force via the pneumatic regulator with a loop rate of 100 Hz. A clear acrylic sheet was used as the counter face of the sensored grasper to enable optical tracking of the tissue simulant deformation using a video extensometer (AVE2, Instron), which was analysed using Digital Image Correlation (DIC) software (GoM Correlate, GoM), images were captured at 50 Hz.

B. Experimental Parameters

Test parameters were defined to emulate regimes used in surgical practice and thus analyse the system over a range of representative conditions exploring the effects of retraction speed, tissue (mechanical) properties and grasping force. Retraction speeds of 1, 2 and 3 mm/s were selected based on those used for tissue manipulation [21], and two different stiffness tissue simulants Mat A (241 kPa) and Mat C (610 kPa) were analysed which had similar tensile elastic properties to liver tissue [22]. These tissue simulants consisted of three layers of silicone elastomer (Ecoflex 00-30, Smooth-on) reinforced with two layers of stretchable spandex fabric between them, 0.3 mm below the upper and lower surfaces. Samples were laser cut to form a 100 × 20 × 3 mm sample. The tensile stiffness of different sample types was controlled through the choice of reinforcement fabric while the elastomer remained the same to provide comparable frictional and compressive properties. A speckle pattern was applied to one side of the simulant using enamel spray paint for tracking the displacement via DIC, and a layer of surfactant lubricant was used to emulate the serous fluid coating many soft tissues [23]. Grasping loads were varied between 10 N and 30 N based on typical pressures reported for surgical grasping of soft tissues [24], [25]. The automated grasping system was compared to a baseline case using a fixed 30 N grasping force. The automated grasping system used an initial grasp force of 10 N to hold the tissue at the start of retraction with a 30 N upper limit (to match the baseline case). Tests were conducted to explore this experimental matrix in which 5 repeats were conducted for each unique configuration (2 control methods, 3 retraction speeds, 2 tissue simulants).

A secondary test was employed to assess the ability of automated system to retract and then hold tissue. The tissue simulant was grasped, then two cycles of retraction (by 1.5 mm) followed by a hold were performed before a final retraction to the point of macro slip. 5 repeats where conducted for each test condition (2 control methods, 2 tissue simulants).

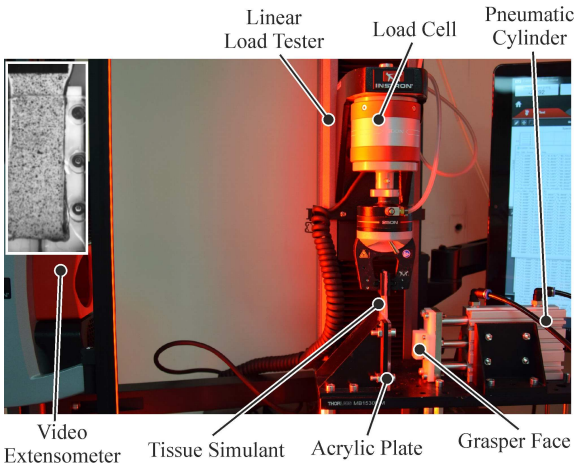

Fig. 6: Image of the experimental set up used for simulating surgical grasping. Inset shows view of tissue simulant from video extensometer.

C. Data processing

To compare the performance of the automated and fixed grasp methods, metrics were defined to capture the peak shear force achieved (i.e. representing the grasp holding performance) and the grasping energy used to achieve this outcome. For the latter, the impulse applied to the tissue simulant during grasping was calculated as a good indicator which relates to the probability of causing tissue trauma [26]. The Impulse (I) was calculated as follows,

$$I = \int_{t=0}^{t=M} F_c \, dt \tag{5}$$

where $t = 0$ is the start of retraction and $t = M$ is the time at which macro slip occurs as determined from the shear force (F_s).

$$\textbf{if } \frac{dF_s}{dt} < 0.025 V_s, \; t = M \tag{6}$$

D. Results

Figure 7 displays representative examples of the applied grasping forces and resultant shear forces for the automated and fixed grasper control methods for all the test conditions investigated.

Both control methods showed a similar pattern for the variation in shear force during the retraction process across all test cases, in which shear gradually increases as the tissue simulant is stretched until the point of global slip, as indicated on the graph. The automated system applies increasing grasp force as the shear force increases to maintain grip stability. This results in similar levels of maximum shear achieved for both methods as well as similar times of macro slip. These aspects are summarised in Figure 8 which shows the peak

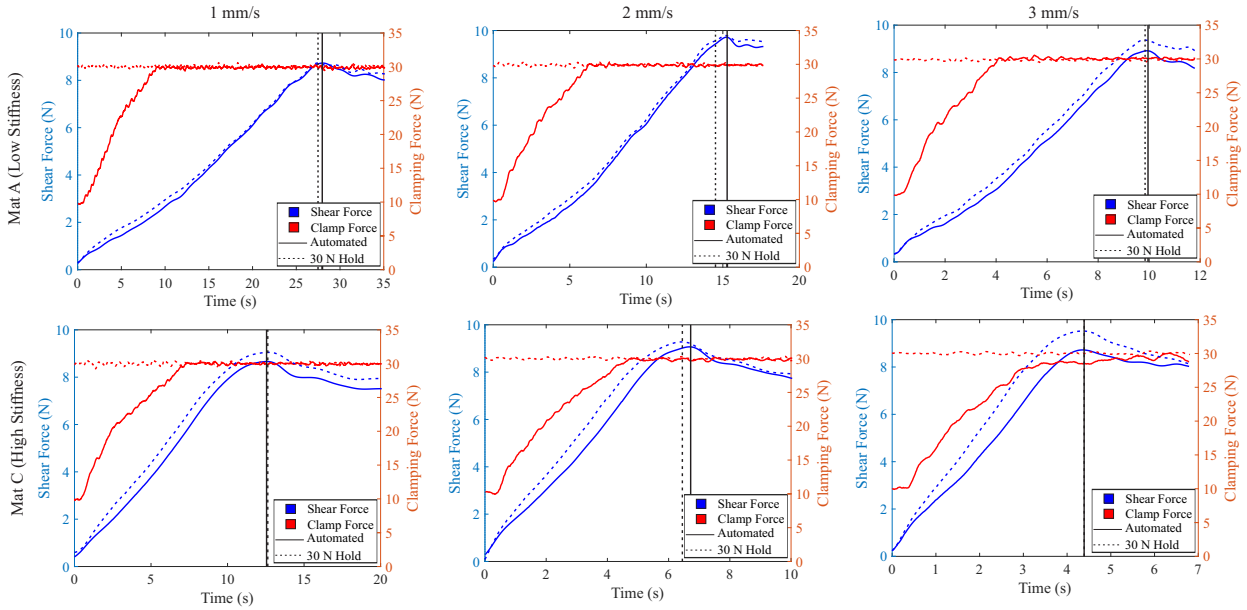

Fig. 7: Typical grasping characteristics recorded for the automated and fixed test cases for variations in tissue simulant material stiffness and grasper retraction speed. Vertical lines indicated the point of macro slip.

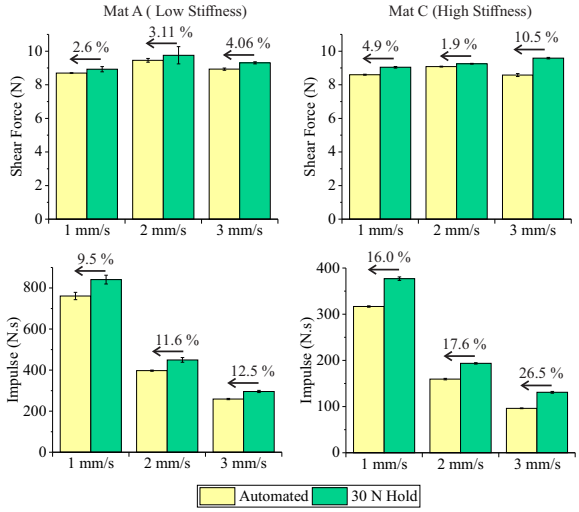

Fig. 8: Summary of the results for the average maximum shear force and average impulse, between t=0 and the point of macro slip, across all test conditions. The percentages indicate the relative decrease in metric between the 30N hold and automated test cases.

shear force and grasping impulse, up to the onset of macro slip.

Statistically significant differences (P<0.05) were observed for the outcome measures when comparing the two control methods (excluding peak shear for Mat A at 2 mm/s). However, the maximum shear force observed using the automated control method was only marginally lower than for the fixed 30 N grasp case, but this was achieved with a substantial decrease in the Impulse applied to the tissue simulant. These differences were more profound for the higher stiffness material (Mat C).

Figure 9 examines the mechanics underlying this process, showing the deformation of the tissue simulant at the front, centre and rear of the grasper (see Fig. 2 for reference) as determined by the video extensometer and DIC analysis. For both the high and low stiffness tissue simulants, the automated control method shows similar behaviour to the fixed load grasp case, particularly at the centre and rear of the grasper. The tissue at the front islands slips slightly more in the automated case, with a peak difference of approximately 0.9 mm occurring during the early stages of retraction, reducing as the system increases towards maximum grasping load.

For 'retract and hold' procedures Figure 10 shows a typical response produced by the system in automated and fixed hold cases. While similar grasp forces are observed throughout the process, the automated case achieves this using significantly lower clamp forces for the majority of the retraction.

IV. Discussion

From the results gathered in this investigation it is evident that engineering a grasper to promote and detect incipient slips provides an effective basis for a system which conservatively regulates grasping force to prevent macro slip of tissue whilst minimising the applied grasp force during retraction.

Comparison of the shear forces required to induce macro slip in the automated and non-automated cases show less than 5% difference for the majority of cases despite significant variations in the material properties of the tissue simulant and the retraction speed applied (Fig. 8). The exception to this is the condition using a high stiffness material under a high retraction speed, where the automated system slips at 10.5% less shear load. This occurs when the grasp force plateaus before reaching the maximum load of 30 N because slip propagates rapidly through the material, such that slip occurs before mitigating action can be taken. This could be addressed by tuning either the automated controller gain (K) or the target slip ratio (ϕ_T), which requires a balance to be made between how rapidly the system responds versus its ability to minimise clamping force. Stiffer materials generally need higher gain and/or ϕ_T (lower bound) values to prevent slip

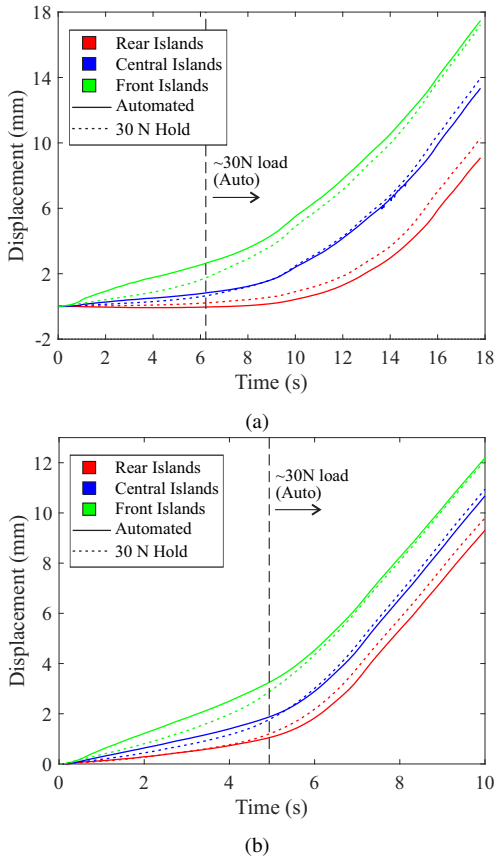

Fig. 9: Representative displacement data for the tissue over the front, central and rear sections of the grasper, for the automated and non-automated control methods. The dashed vertical line indicates the point at which the automated system reaches the maximum 30N clamp force. (a) Low stiffness simulant (Mat A) with a 2mm/s retraction speed. (b) High stiffness simulant (Mat C) with a 2mm/s retraction speed.

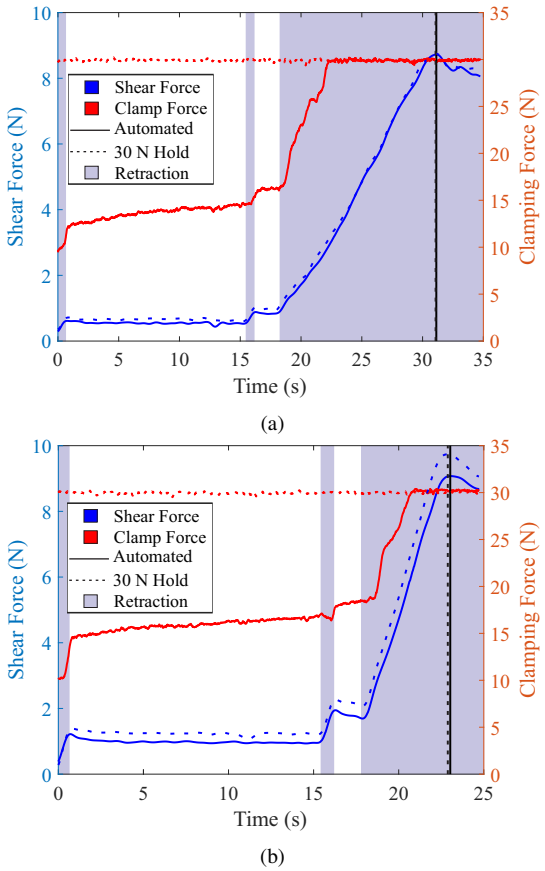

Fig. 10: Typical force characteristics during a retract and hold of tissue simulant for: (a) Low stiffness simulant (Mat A). (b) High stiffness simulant (Mat C). The black vertical lines indicate the point of macro slip, whilst the purple shaded areas indicate when the tissue is being retracted at 2 mm/s.

occurring as they need either a faster (K) or earlier (ϕ_T (lower bound)) response to incipient slip events (Fig. 5), however after a certain point further increases in these values provides no further benefit to the system in preventing slip but will result in higher clamp forces being applied prematurely.

Using impulse as an indicator of the energy applied to the tissue simulant demonstrates that the automated control method brings a significant reduction in potential tissue trauma, especially in cases using the high stiffness tissue simulant. The sensor islands are positioned at the front edge of the graper so they detect when slip occurs at that front edge and initiate a mitigating reaction. For high stiffness tissue, the front and rear of the grasper slip almost simultaneously [17], so the grasper reaches the maximum clamp load shortly before macro slip occurs, minimising the force applied over the retraction (Fig. 7). For the low stiffness material the slip propagation from front to back occurs more gradually, so there is a significant amount of time before the tissue at the rear slips and the automated system remains at maximum load for longer resulting in less improvement in the impulse applied.

The differing performance (in terms of both grasp and input energy) for the automated system across the test cases suggests that there will be limitations in the operating conditions and tissue properties for which it is suitable. However, the current results do demonstrate a wide operating range which does not require tissue-specific thresholding methods for effective operation, a key to making these techniques more broadly applicable in surgical settings. The sensors performance could also be improved by utilising an additional row of sensors at the rear of the grasper, enabling comparison of island movements between the grasper's front and rear, enabling an estimation of material stiffness and the speed of slip propagation. Both of these attributes could then be fed into the control system to optimise grasp force accordingly.

The tissue deformation under grasping observed using DIC techniques further validates the efficacy of the incipient sensing approach and the automated control method, as for both materials there is a high correlation between the automated and fixed grasp results. During the initial retraction period there is slightly more displacement at the front islands when using the automated case as less clamp force is being applied. However the adjustment made by the automated system prevents the slip propagating any faster than in the fixed hold case, resulting in near identical grasping performance, despite significantly reduced load being applied to the tissue simulant during this manoeuvre.

The system has also been demonstrated to perform effectively when conducting a 'retract and hold' of the tissue simulant, resulting in similar holding performance with sig-

nificantly lower clamping forces compared to a fixed load approach (see Fig 10). A gradual increase is evident in the clamping force during the hold phase, a result of sensor noise on the velocity measurements causing small incremental increases in force, though further refinement of the current algorithm is being developed to mitigate these effects. However, the results presented here for short grasp and retract procedures represent those in which the system could provide the most benefit; in shorter retractions only a fraction of the maximum possible clamp force is required to prevent slip, therefore the automated grasping system presented here could enable a significant reduction in the overall clamp forces applied, reducing the probability of causing tissue damage due to the over application of force [2], [26].

V. Conclusions and further work

This study demonstrates the efficacy of using a segmented incipient slip sensor as the basis for improving automated grasping of soft tissues in surgery during tissue retraction. Results from evaluation of the system show this method provides the possibility for improving surgical outcomes by reducing the forces applied to tissues during retraction whilst still maintaining a similar gripping performance to using a maximumal grasping force. The system proved capable over a range of materials and retraction speeds representative of surgical conditions, though the results indicate there will be limitations to the range of materials for which system will provide a performance benefit. Analysis of the system performance highlighted how the system can be further developed to broaden its operating range. Further work will consider evaluation of the system performance in ex-vivo tissue samples and working to miniaturise the sensing technology for future integration into a surgical grasper.

References

[1] D. M. Herron and M. Marohn, "Prepared by the SAGES-MIRA Robotic Surgery Consensus Group," p. 24, 2006.

[2] B. Tang, G. Hanna, and A. Cuschieri, "Analysis of errors enacted by surgical trainees during skills training courses," *Surgery*, vol. 138, no. 1, pp. 14–20, Jul. 2005.

[3] E. Heijnsdijk, J. Dankelman, and D. Gouma, "Effectiveness of grasping and duration of clamping using laparoscopic graspers," *Surgical Endoscopy*, vol. 16, no. 9, pp. 1329–1331, Sep. 2002.

[4] C.-H. King, M. Culjat, M. Franco, C. Lewis, E. Dutson, W. Grundfest, and J. Bisley, "Tactile Feedback Induces Reduced Grasping Force in Robot-Assisted Surgery," *IEEE Transactions on Haptics*, vol. 2, no. 2, pp. 103–110, Apr. 2009.

[5] C.-H. King, M. Culjat, M. Franco, J. Bisley, G. Carman, E. Dutson, and W. Grundfest, "A Multielement Tactile Feedback System for Robot-Assisted Minimally Invasive Surgery," *IEEE Transactions on Haptics*, vol. 2, no. 1, pp. 52–56, Jan. 2009.

[6] V. Nitsch and B. Farber, "A Meta-Analysis of the Effects of Haptic Interfaces on Task Performance with Teleoperation Systems," *IEEE Transactions on Haptics*, vol. 6, no. 4, pp. 387–398, Oct. 2013.

[7] N. T. Burkhard, J. Ryan Steger, and M. R. Cutkosky, "The Role of Tissue Slip Feedback in Robot-Assisted Surgery," *Journal of Medical Devices*, vol. 13, no. 2, p. 021003, Jun. 2019.

[8] G.-Z. Yang, J. Cambias, K. Cleary, E. Daimler, J. Drake, P. E. Dupont, N. Hata, P. Kazanzides, S. Martel, R. V. Patel, V. J. Santos, and R. H. Taylor, "Medical robotics—Regulatory, ethical, and legal considerations for increasing levels of autonomy," *Science Robotics*, vol. 2, no. 4, p. eaam8638, Mar. 2017.

[9] S. M. Khadem, S. Behzadipour, A. Mirbagheri, and F. Farahmand, "A modular force-controlled robotic instrument for minimally invasive surgery - efficacy for being used in autonomous grasping against a variable pull force: Modular force-controlled robotic instrument," *The International Journal of Medical Robotics and Computer Assisted Surgery*, vol. 12, no. 4, pp. 620–633, Dec. 2016.

[10] D. Jones, A. Alazmani, and P. Culmer, "A Soft Inductive Tactile Sensor for Slip Detection Within a Surgical Grasper Jaw," p. 4, 2019.

[11] N. T. Burkhard, M. R. Cutkosky, and J. R. Steger, "Slip Sensing for Intelligent, Improved Grasping and Retraction in Robot-Assisted Surgery," *IEEE Robotics and Automation Letters*, vol. 3, no. 4, pp. 4148–4155, Oct. 2018.

[12] K. L. Johnson, *Contact mechanics*. Cambridge Cambridgeshire New York: Cambridge University Press, 1987.

[13] J. Stoll and P. Dupont, "Force Control for Grasping Soft Tissue," p. 4, May 2006.

[14] W. Chen, H. Khamis, I. Birznieks, N. F. Lepora, and S. J. Redmond, "Tactile Sensors for Friction Estimation and Incipient Slip Detection – Towards Dexterous Robotic Manipulation: A Review," *IEEE Sensors Journal*, pp. 1–1, 2018.

[15] M. Tremblay and M. Cutkosky, "Estimating friction using incipient slip sensing during a manipulation task," in *[1993] Proceedings IEEE International Conference on Robotics and Automation*. Atlanta, GA, USA: IEEE Comput. Soc. Press, 1993, pp. 429–434.

[16] F. Veiga, J. Peters, and T. Hermans, "Grip Stabilization of Novel Objects using Slip Prediction," *IEEE Transactions on Haptics*, pp. 1–1, 2018.

[17] I. Waters, A. Alazmani, and P. Culmer, "Engineering incipient slip into surgical graspers to enhance grasp performance," *IEEE Transactions on Medical Robotics and Bionics*, pp. 1–1, 2020.

[18] H. Khamis, R. Izquierdo Albero, M. Salerno, A. Shah Idil, A. Loizou, and S. J. Redmond, "PapillArray: An incipient slip sensor for dexterous robotic or prosthetic manipulation – design and prototype validation," *Sensors and Actuators A: Physical*, vol. 270, pp. 195–204, Feb. 2018.

[19] J. C. Norton, J. H. Boyle, A. Alazmani, P. R. Culmer, and A. Neville, "Macro-Scale Tread Patterns for Traction in the Intestine," *IEEE Transactions on Biomedical Engineering*, vol. 67, no. 11, pp. 3262–3273, Nov. 2020.

[20] D. Jones, L. Wang, A. Ghanbari, V. Vardakastani, A. E. Kedgley, M. D. Gardiner, T. L. Vincent, P. R. Culmer, and A. Alazmani, "Design and Evaluation of Magnetic Hall Effect Tactile Sensors for Use in Sensorized Splints," *Sensors*, vol. 20, no. 4, p. 1123, Feb. 2020.

[21] A. Alazmani, R. Roshan, D. G. Jayne, A. Neville, and P. Culmer, "Friction characteristics of trocars in laparoscopic surgery," *Proceedings of the Institution of Mechanical Engineers, Part H: Journal of Engineering in Medicine*, vol. 229, no. 4, pp. 271–279, Apr. 2015.

[22] A. R. Kemper, A. C. Santago, J. D. Stitzel, J. L. Sparks, and S. M. Duma, "Biomechanical Response of Human Liver in Tensile Loading," p. 12, Jan. 2010.

[23] W. Schwarz, "The surface film on the mesothelium of the serous membranes of the rat," *Zeitschrift fr Zellforschung und mikroskopische Anatomie*, vol. 147, no. 4, pp. 595–597, 1974.

[24] A. W. Brown, S. I. Brown, D. Mclean, Z. Wang, and A. Cuschieri, "Impact of fenestrations and surface profiling on the holding of tissue by parallel occlusion laparoscopic graspers," *Surgical Endoscopy*, vol. 28, no. 4, pp. 1277–1283, Apr. 2014.

[25] P. Mucksavage, D. C. Kerbl, D. L. Pick, J. Y. Lee, E. M. McDougall, and M. K. Louie, "Differences in Grip Forces Among Various Robotic Instruments and da Vinci Surgical Platforms," *Journal of Endourology*, vol. 25, no. 3, pp. 523–528, Mar. 2011.

[26] A. I. Margovsky, R. S. A. Lord, and A. J. Chambers, "The effect of arterial clamp duration on endothelial injury: An experimental study," *ANZ Journal of Surgery*, vol. 67, no. 7, pp. 448–451, Jul. 1997.